ACS APPLIED MATERIALS & INTERFACES

www.acsami.org

Research Article

Using Hybrid Coating to Fabricate Highly Stable and Expandable Transparent Liquid Marbles

Renis Agosto Nieves, Gabriela Gomez Dopazo, Joseph Rosenfeld, Hong-Huy Tran, Lyanivette Alvarado Lopez, Jose Sotero-Esteva, Ezio Fasoli, Ivan J. Dmochowski, Daeyeon Lee, and Vibha Bansal*

Cite This: *ACS Appl. Mater. Interfaces* 2024, 16, 68336−68347

Read Online

ACCESS | Metrics & More | Article Recommendations | Supporting Information

ABSTRACT: Liquid marbles (LMs) are microliter-scale droplets coated with hydrophobic solid particles. The particle size and hydrophobicity of the surface coating determine their properties, such as transparency, expandability, and resistance to evaporation and coalescence, one or more of which can be critical to their application as microreactors. This study reports the use of a mixture of two different hydrophobic powders for fabrication of LMs for colorimetric assays: trichloro(1*H*,1*H*,2*H*,2*H*-perfluorooctyl) silane-linked silica gel (modified silica gel (MSG), particle size: 40−75 μm) and hexamethyldisilazane-linked fumed silica (modified fumed silica (MFS), average aggregate length: 200−300 nm). The hybrid coating mixture (MIX) prepared by mixing these MSG and MFS powders in a ratio of 3:7 (w/w), respectively, contained particles of different sizes as well as different hydrophobicity as the silane linked to MSG is more hydrophobic than the one linked to MFS. LMs fabricated using MIX as the surface coating were characterized and compared to LMs coated with MSG or MFS alone. It was observed that MIX LMs were comparable to the MFS LMs in transparency (higher than the MSG LMs), expandability (more than 20 times their initial volume), and stability against evaporation (for more than 4 h at 78% relative humidity at 26 °C). However, in terms of resistance to coalescence, the MIX LMs showed a resistance comparable to that of MSG LMs, much higher than that of MFS LMs. Further experiments demonstrated that it is the presence of the particles of different sizes (MSG particles are ∼100 times larger than MFS) that improves the resistance to coalescence rather than the higher hydrophobicity of the MSG. Three different colorimetric assays were performed in the MIX LMs, and the results obtained were comparable in accuracy and precision to those obtained in a standard polystyrene microwell plate system. Low quantities of the analytes could be detected and quantified, as evidenced by the limit of detection (alkaline phosphatase (AP): 0.18 μg/mL; bovine serum albumin (BSA): 2.28 μg/mL; and chymotrypsin: 3.69 μM) and limit of quantification (AP: 0.59 μg/mL; BSA: 12.29 μg/mL; and chymotrypsin: 7.59 μM) values. Color intensities in LMs were quantified using a smartphone application, which provides the added benefit of an instrument-free approach. These findings highlight the potential of using LMs stabilized with mixtures of nano- and microparticles as robust, versatile microreactors for portable and sensitive colorimetric assays, paving the way for more accessible and efficient diagnostic tools.

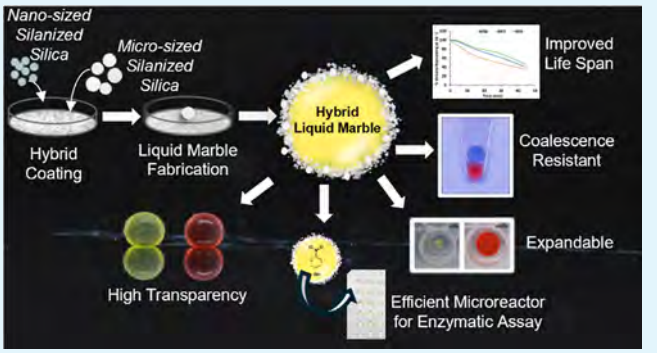

KEYWORDS: *colorimetric methods, hydrophobic coatings, evaporation time, coalescence, silanized silica gel, silanized fumed silica, hybrid coating, microreactor*

INTRODUCTION

Liquid marbles (LMs) are self-standing microliter droplets stabilized by hydrophobic particles that self-organize at the liquid/air interface[1,2] into a densely packed shell. Coated droplets (LMs) thus formed are stable, manipulable, and even resistant to coalescence with neighboring LMs depending upon the particles used.[1,3−7] These features enable the transport of small quantities of core liquids without loss of mass or cross contamination.[8,9] The flexibility and self-healing properties of LMs allow injection of secondary reagents to perform reactions, making them excellent microreactors.[3,4,7] In addition, LMs form important tools for reducing waste generation and reagent usage in laboratories due to their small volumes which also facilitates expedited reaction times.[4,8,10] All these characteristics of LMs have led to their being studied for wide-ranging applications[4,11−14] that include

Received: September 3, 2024
Revised: November 6, 2024
Accepted: November 19, 2024
Published: November 27, 2024

https://doi.org/10.1021/acsami.4c14949
ACS Appl. Mater. Interfaces 2024, 16, 68336−68347

cell culture reactors,[5,15−17] micropumps,[12] pH indicators,[13] oily wastewater sensors,[18] gas sensors,[19] and vessels to form in vitro embryoid bodies.[11]

One interesting application of LMs has been for colorimetric applications that range from sensors for field jobs to biomedical diagnostic devices.[4,10,20,21] Effective colorimetric analyses in LMs require that the LMs be transparent, stable for the duration of the analysis, and resistant to coalescence. All of these characteristics of the LMs are determined by the surface coatings. For example, coatings containing nanoparticles such as fumed silica (FS) (typically smaller than 50 nm) yield transparent LMs as opposed to hydrophobic coatings containing micrometer-sized particles[5,15,22−24] but these LMs tend to undergo coalescence when they come into contact with each other. Mixing FS with silicone oil leads to a surface coating that yields LMs with improved resistance to coalescence.[25] These LMs, known as composite LMs, combine the advantages of silicone oil and FS coatings. It has also been shown that the lifetime and stability of LMs can be manipulated by varying the coating particle size[26,27] and hydrophobicity,[2,28,29] respectively; however, correlations between these properties have not been clearly established. Stability of LMs against coalescence and evaporation is important for other potential applications, such as bioreactors. LMs that do not coalesce instantaneously[30] form important tools in processes where controlled coalescence using external energy is required or where coalescence is entirely detrimental to the application. For example, noncoalescing transparent LMs have the potential to be used as cell culture beads inside reactors while also allowing real-time monitoring of cell growth. Stacking of LMs and storage for later use in analyses outside or inside laboratories are also possible if they are resistant to coalescence. Resistance to evaporation is also an important feature as most colorimetric assays and cell cultures require reaction times ranging from 5 to 30 min and beyond and temperatures frequently up to at least 37 °C. Water inside the LMs, though slightly slower than a bare liquid droplet, does evaporate easily, causing LMs to have short lifetimes even at moderate temperatures.[31] The rate of evaporation of LMs varies, depending upon the particle size, surface energy, and hydrophobicity of the powder. Thus, factors such as particle size, hydrophobicity of the surface coating, and the number of layers of powder on the LM surface hold key to fabrication of LMs with desired features for a specific application.

In this study, we report a mixture of two different powders as surface coating to fabricate LMs without limitations imposed by either of these coatings individually. Transparent LMs were fabricated using a hybrid coating composed of two powders consisting of particles of different sizes and hydrophobicity: (i) modified fumed silica (MFS): relatively small particles (200−300 nm) of FS modified with hexamethyldisilazane (available commercially); (ii) modified silica gel (MSG): larger particles of SG (40−75 μm) modified with trichloro(1*H*,1*H*,2*H*,2*H*-perfluorooctyl) silane (TFOS). LMs coated with MFS only were highly transparent but coalesced easily. While the LMs formed using only MSG possessed lower transparency and half-life, they were resistant to coalescence. LMs were then fabricated using the mixture of these two powders in different ratios. A 3 MSG:7 MFS (w/w) mixture (to be referred to as MIX) led to LMs with properties superior to those of LMs composed of either of the two powders alone. The three different types of LMs (MSG, MFS, and MIX) were characterized for transparency, stability at different temperatures, and expandability. The MIX LMs are injectable with analyte solution using a glass syringe or a pipet fitted with the polypropylene tip and highly expandable (>20 times their original volume). The transparency coupled to their injectability and expandability makes them ideal for colorimetric estimation of enzyme activity and protein concentration. The MIX LMs were used for colorimetric assays using a commercially available smartphone application for measuring color intensity inside the LMs. Analysis of the observed differences in transparency and stability among various LMs, in relation to the particle size and hydrophobicity of the applied coatings, provides valuable insights into how the physicochemical properties of LMs can be tuned by using mixtures of particles for specific applications.

EXPERIMENTAL SECTION

Materials and Reagents. All reagents used were of ACS grade and purchased from Millipore Sigma (USA). Surface modification of SG (particle size: 40−75 μm) was performed using ethyl alcohol (≥99.5% purity), ammonium hydroxide solution (≥20−<30%), and TFOS (≤100%). FS treated with a hexamethyldisilazane, CAB-O-SIL TS-530 (referred to as MFS in this article, average aggregate length: 200−300 nm), was obtained as a donation from Cabot Corporation (Alpharetta, Georgia, USA).

Spotxel Reader. Plate Reader & Microarray Image Analysis, a free application (app) available in the App Store and Google Play (https://www.sicasys.de/spotxel-reader/), was used for quantification of color intensities in colorimetric assays performed inside the LM. This app can be downloaded and used on smartphones (both Apple and Android) and Windows computers. The app works by analyzing the image of the microwell plate containing the reaction mixtures. The image can be taken in the app as well as imported into the app. The wells need to be aligned with the virtual plate template in-app, and the app then reports color intensity values for each well. In this study, iPhone main cameras with a resolution of 12 MP (https://www.apple.com/iphone/compare/?modelList=iphone-11,iphone-13,iphone-14-plus) were used to capture images of the assays. This type of smartphone was chosen for convenience. The images were taken at an optical zoom of 1×.

Absorbance in colorimetric assays performed in Greiner 96-well polystyrene plates (Millipore Sigma) was measured with an Epoch Microplate Spectrophotometer (Agilent Technologies). MSG particle washes were monitored using a NanoDrop 2000 Spectrometer (Thermo Scientific). The relative humidity (RH) and temperature were measured with an AcuRite Indoor Digital Thermometer & Hygrometer with temperature and humidity.

Fabrication of LMs. *Surface Modification of SG.* First, 0.1 g of TFOS and 0.2 g of silica were added to a solution containing 12.0 mL of ethyl alcohol and 345 μL of ammonium hydroxide. This reaction mixture was stirred vigorously for 40 min.[32] SG modified with TFOS will henceforth be termed MSG. The MSG was dried in a vacuum oven (22 in Hg) at 65 °C for 5 h. To confirm the modification of the SG with TFOS, both SG and MSG were analyzed using ATR-FTIR spectroscopy (Nicolet iS10 FTIR Spectrometer equipped with a mid-infrared Ever-Glo and tungsten halogen lamp, Thermo Fisher Scientific). ATR-FTIR spectra were recorded between 400 and 4000 cm^{-1} with a spectral resolution of 0.4 cm^{-1}, and 16 scans were collected.

Preparation of the Hydrophobic Coating Mixture. A mixture (MIX) of MSG and commercially available MFS (CAB-O-SIL) was prepared by mixing these two powders in a ratio of 3:7 (w/w), respectively.

Surface Modification of FS. Surface modification of FS was performed following a published protocol.[33] FS (1.5 g), which had previously been dried at 120 °C for 24 h in a vacuum oven, was reacted with TFOS (2.0 g) in toluene (50.0 mL). This reaction mixture was stirred vigorously at 50 °C for 24 h. The TFOS-linked MFS was finally vacuum filtered and dried in a vacuum oven (22 in

https://doi.org/10.1021/acsami.4c14949
ACS Appl. Mater. Interfaces 2024, 16, 68336−68347

Hg) at 150 °C for 5 h. To confirm the modification of the FS with TFOS, both FS- and TFOS-linked MFS were analyzed using ATR-FTIR spectroscopy (Nicolet iS10 FTIR Spectrometer equipped with a mid-infrared Ever-Glo and tungsten halogen lamp, Thermo Fisher Scientific). ATR-FTIR spectra were recorded between 400 and 4000 cm^{-1} with a spectral resolution of 0.4 cm^{-1}, and 16 scans were collected. FS modified with TFOS will henceforth be termed T8-MFS (TFOS MFS).

Preparation of LMs. LMs were fabricated by rolling a droplet (of desired size) of the relevant solution[3,34] on a bed of the prepared hydrophobic particle mixture (MSG or MFS or MIX). The LMs were transferred to the appropriate vessel with a plastic spatula. LMs, formed with 10 μL of yellow-colored deionized water (DW) using each of the three coatings, were examined using an Olympus SZ61 dissection microscope at a magnification of 15×.

Characterization of LMs. *Coalescence.* The ease of coalescence of LMs was studied by placing multiple LMs together in a microcentrifuge tube and/or Petri plate and observing their fusion.

Stability at Different Temperatures (4 °C, 37 °C, and RT). LMs, prepared with each of the three coatings, MSG, MFS and MIX, were placed at different temperatures, 4 °C, 37 °C, and RT (26 °C) and monitored for evaporation over extended time intervals. The RT studies were carried out under two different humidity (RH) conditions: 48% and 78%. Images and videos were taken throughout the observation period using a Cannon EOS Rebel T4i camera fitted with an EFS 18−55 mm lens. ImageJ/FIJI software (https://imagej.net/software/fiji/downloads) was used to measure the cross-sectional area and height of the LMs in the pictures taken at different time points (0−45 min every 15 min). Assuming that the LMs have axial symmetry, the volume of a rotated shape formula was used

$$\text{volume} = \pi \times \text{cross} - \text{sectional area} \times \text{height} \quad (1)$$

to calculate the volume of the LMs at each point. To compare the rate of change in volume for differently coated LMs, % volume remaining at any given time for each LM was then calculated using the formula shown in eq 2.

$$\%\ \text{volume remaining at time } (t) = \frac{\text{volume at time } (t)}{\text{volume at time zero}} \times 100 \quad (2)$$

Injectability and Expandability. DW was colored by adding a few drops of yellow or red food color to facilitate observation of marble expansion. LMs occupying individual microwells and containing yellow-colored DW containing LM (5 μL) were injected with red-colored DW until they collapsed or expanded enough to fill up the microwell. Injections were performed using a 0.2−10 μL micropipette with a regular pipet tip (made of polypropylene). LMs were carefully inspected for structural integrity after each injection.

Optical Characterization. The effect of surface coating on the transparency of LMs was studied both qualitatively and quantitatively.

Qualitative Estimation. Each of the three coatings (MSG, MFS, and MIX) was used to prepare one red-colored and another yellow-colored DW containing LM. The two LMs of each coating were placed in front of each other or side by side. The resulting reflection of colors between the two LMs was used to analyze their transparency qualitatively.

Quantitative Measurement of Transparency. The transmittance of light through LMs is affected by the surface coating particles. Hence, the coating composition determines the transparency of the LM.[5,15] The effect of each coating (MSG, MFS, and MIX) on transmittance of light through the LMs fabricated in this study was quantified through ImageJ analysis of the images of three different LMs of each coating taken against a blue background with the iPhone 15 camera in a controlled illumination box. The images were in HEIC format (3024 × 4032 pixels, RGB). Sample regions were selected from the (blue) background of the image and from the center of the LMs (100 × 100 and 80 × 80 pixels, respectively). In both cases, areas with specular reflections were avoided. In the case of LMs, an area as close as possible to the center was selected. In the case of the background, an area close to the marble with the x coordinate similar to that of the marble sample was selected. RGB values of the background and different LM samples were computed as triples (r_{bg}, g_{bg}, b_{bg}) and (r_m, g_m, b_m).[35] The background color was subtracted from the marble color to remove the contribution of the surface to the visible color. The resulting triplet was then used to compute the vector norm as shown in eq 3.[36]

$$\text{Transmittance} = 1 - \frac{1}{3}\sqrt{(r_m - r_{bg})^2 + (g_m - g_{bg})^2 + (b_m - b_{bg})^2} \quad (3)$$

A higher transmittance indicates a greater transparency of the marble. The *Python* interpreter v.3.12.3 with *NumPy* v.1.26.4[37] and the *Pillow Python Imaging Library* v.10.2.0 was used to analyze the images.

Colorimetric Assays. The usability of LMs as microreactors for colorimetric estimations was demonstrated by performing three different assays using standard protocols: (i) bicinchoninic acid assay (BCA) for protein quantification;[38] (ii) alkaline phosphatase (AP) assay based on hydrolysis of *p*-nitrophenyl phosphate (PNPP);[39] and (iii) chymotrypsin (CT) assay based on the hydrolysis of *N*-succinyl-Ala-Ala-Pro-Phe-*p*-nitroanilide (SAAPPpNA),[40] using standard protocols.

LMs in Cellulose Acetate Microwell Plates. Multiwell plates (96-well) were prepared in our laboratory using cellulose acetate (CA).[41] These plates are white opaque and in the same format as corresponding 96-well polystyrene plates. The LMs were fabricated for colorimetric assays using a solution containing all reagents (substrate, buffer, etc.) except the analyte (protein or enzyme). LMs were then placed in the 96-well CA plates with conical wells. The colorimetric reaction was started in each case by injecting the enzyme or protein solution into the LMs using a micropipette fitted with a regular micropipette tip. The resulting color formation in the LMs was quantified using a smartphone application (available for free), Spotxel Reader: Plate Reader & Microarray Image Analysis.

Plastic Microwell Plates. The results obtained with LMs in CA plates and the Spotxel Reader were compared to the same assays performed in the traditional polystyrene microwell plates and the microplate reader system. Absorbances in polystyrene microwell plates were read by using a microwell plate reader at wavelengths of 562 nm (BCA), 405 nm (AP), and 410 nm (CT). All measurements were performed in triplicate, and the assays were repeated at least three separate times.

RESULTS AND DISCUSSION

The potential of LMs for a wide range of applications is evident from the significant amount of scientific literature that has been published in the last two decades.[5,12,17,20,42] As the surface coatings determine the different features of LMs such as stability and transparency, an informed preparation of these coatings is vital to the integration of LMs into larger-scale processes. In this study, we report the use of a mixture of two powders of different particle sizes and hydrophobicity to fabricate LMs that combine desirable traits from each coating. The applicability of these LMs as biochemical reactors was demonstrated by performing three colorimetric assays in them.

Fabrication of LMs. A commercially available silanized FS, CAB-O-SIL TS-530 (referred to in this study as MFS) containing amorphous particles of average aggregate size in the range of 200−300 nm, has been used by other researchers to fabricate transparent LMs.[43] Since using LMs for colorimetric methods requires LMs to be transparent, starting this study with MFS constituted a logical choice. Although LMs formed using this MFS showed high transparency, they instantly coalesced with other LMs (Figure 1A; video of coalescence of the MFS LMs has been provided in Supporting Information, S1). This spontaneous coalescence ruled out the facility of

https://doi.org/10.1021/acsami.4c14949
ACS Appl. Mater. Interfaces 2024, 16, 68336−68347

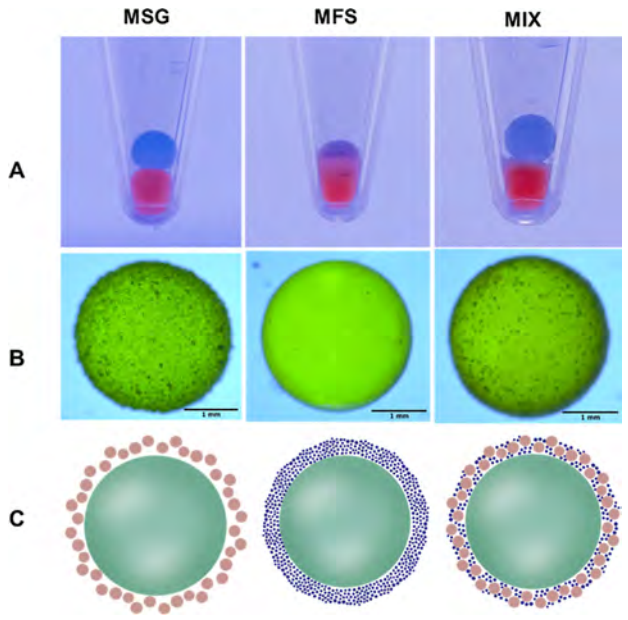

Figure 1. Surface properties of LMs made using the MSG, MFS, and MIX coatings (in order from left to right). (A) Resistance of LMs to coalescence due to stacking: a blue-colored-water-containing LM was placed on top of a red-colored LM in a 500 μL microcentrifuge tube. The second LM can be seen fused to the first one in case of the MFS LM-containing tube, while the other two types of LMs (MSG and MIX) stay structurally intact and separated. (B) Morphology of LMs: microscope images (15×) of the MSG LM showed a rugged appearance with big MSG particles appearing to form a dense layer, while the MFS LM shows a very smooth surface making it difficult to see individual particles of MFS. The MIX morphology is in between the other two where a smooth surface coated with MFS is seen with occasional MSG particles distributed scarcely. (C) Cartoon depicting possible arrangement of the three different coatings on the LM surface. The central green circle represents the liquid core of the LM and the dots surrounding this core represent the coating particles.

making and storing several LMs for an experiment in one tube or plate.

Studies have shown that hydrophobic coatings consisting of small particles favor the coalescence of LMs.[44] Hence, SG particles (particle size: 40−75 μm), which are almost 1,000 times bigger than FS (particle size: 200−300 nm), were chemically modified with TFOS[45] as a surface coating for LMs. The linkage of SG to TFOS was confirmed through FTIR spectroscopy of washed and dried hydrophobized SG particles (to be referred to as MSG)[46] (Supporting Information, Figure S1). The LMs rolled in MSG were highly resistant to coalescence (Figure 1A; video of coalescence has been provided in the Supporting Information, S2) but showed limited lifetime at a RH of 48%, as a 10 μL marble started buckling in less than 5 min at RT, 26 °C (video of the evaporation of LM at RT has been provided in Supporting Information, S3). This was in sharp contrast with similarly sized MFS LMs where buckling did not start until 54 min at RT.

Given the trade-off in the stability against coalescence and lifetime of these two types of LMs, mixtures of MFS and MSG were prepared using different ratios (MSG: MFS = 1:1, 1:6, 4:6, and 3:7 w/w) for LM fabrication. The goal was to obtain a highly transparent LM that resisted coalescence. It was observed that the 4 MSG: 6 MFS (w/w) mixture ratio did not resist coalescence, despite the high amount of MSG in the mixture (video of coalescence has been provided in the Supporting Information, S4). The 3 MSG: 7 MFS (w/w) mixture yielded the hydrophobic powder (MIX) that formed LMs with high transparency and stability comparable to MFS LMs, while the resistance to coalescence was similar to that of MSG LMs (Table 1; video of coalescence has been provided in the Supporting Information, S5).

Colorimetric assays were thus performed in LMs prepared with a MIX surface coating. The MSG LM was stable on all surfaces tested (plastic, glass, and metal). However, the MFS and MIX LMs were found to collapse on substrates made of glass, most likely due to the hydrophilic nature of the glass. Therefore, all experiments being reported here were performed in polypropylene microcentrifuge tubes, polystyrene Petri plates, CA microwell plates (designed and fabricated in our laboratory[41]), or metallic surfaces.

Surface Characterization. LMs made with each coating were examined under a microscope to understand the distribution of particles on the surface (Figure 1B). The MFS LMs showed a very smooth surface with individual FS particles difficult to perceive, while the MSG LMs showed a rugged appearance, where individual SG particles could be seen densely packed on the surface. Microscopic imaging of MIX LMs showed the LMs to be coated with MFS and MSG particles, the latter clearly visible but distributed more sparsely than in LMs made entirely from MSG. A cartoon has been included in Figure 1C to depict the coating particle distribution in the different LMs. MSG LM, MFS LM, and the MIX LM can be seen in order from left to right. The MSG LM is coated with the MSG particles, relatively larger in size, forming a dense uneven layer due to the inability of big particles to form a uniform coating. The MFS LM instead is coated with much smaller MFS particles, which form a uniform coating. The MIX LM, while being coated with small MFS particles, has larger MSG particles distributed scarcely throughout the surface.

Table 1. Characteristics of the LM Prepared Using Three Different Hydrophobic Powders

	MSG	MFS	MIX
particle size[a]	40−75 μm	200−300 nm	200−300 nm and 40−75 μm in 3:7 (w/w) ratio
dimensions (w × h) in mm[b]	3.12 × 2.32	2.86 × 2.50	2.86 × 2.50
coalescence	do not coalesce	coalesce	do not coalesce
evaporation time (at ∼25 °C)[c]	40 min (at RH 49%), 4 h 16 min (at RH 78%)	55 min (at RH 49%), 5 h 21 min (at RH 78%)	60 min (at RH 49%), 5 h 19 min (at RH 78%)

[a]Based on the manufacturer-specified size range for each type of coating. [b]Determined with standard deviation in the range of 0.74−1.61%. [c]Measured in triplicate with RSD in the range of 1−5%.

https://doi.org/10.1021/acsami.4c14949
ACS Appl. Mater. Interfaces 2024, 16, 68336−68347

Optical Characterization. It is generally understood that the transparency of LMs is not affected by the hydrophobicity of the coating but by the particle size and the number of layers of coating that forms on the LMs during the rolling of the droplet on the particle bed.[5] MSG particles are approximately 1,000 times bigger than MFS and easily discernible to the naked eye. The three different LMs formed in this study had different levels of transparency. A qualitative estimation of the transparency of these LMs was performed by preparing two LMs with each of the three coatings: one with yellow-colored DW and the other with red-colored DW. The differently colored LMs of each coating were first placed side by side (Figure 2A). Then, the red LM was placed behind the yellow

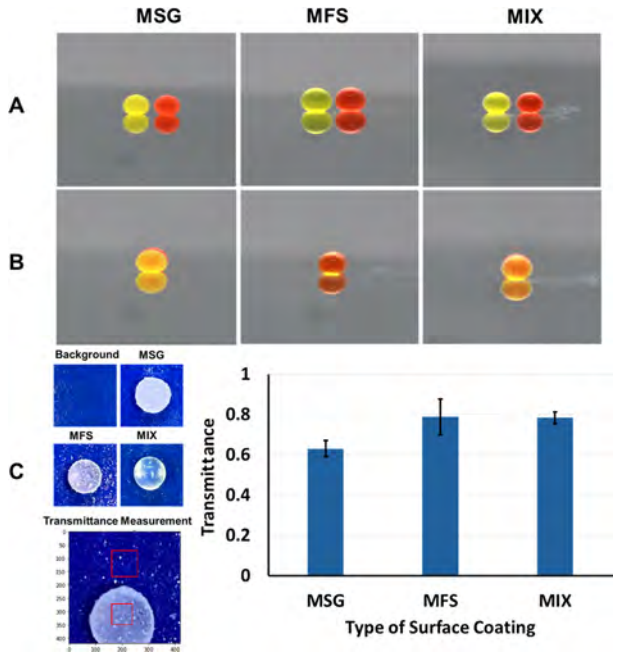

Figure 2. Optical properties of LMs fabricated using three different surface coatings: MSG, MFS, and MIX (in order from left to right). (A) Yellow- and red-colored-water-containing LMs of each coating placed next to each other. (B) Yellow-colored-water-containing LM placed in front of a red-colored LM. Red color of the LM placed in back visible through the yellow LMs placed in front indicates transparency. (C) Quantitative measurements of transparency were performed by preparing LMs with each of the three different coatings using colorless water and placing them against a blue background. Photographs were taken for each LM and sample regions selected in each case from the (blue) background of the image and from the center of the LMs (100 × 100 and 80 × 80 pixels, respectively) as shown by red boxes in the lower-left image. These regions were then analyzed to measure the background blue color transmitted through each LM. Higher transmittance of background (blue) color through the LM, in the graph on the right, indicates higher transparency of the LM.

LM and the color emanating from the yellow LM was observed (Figure 2B). The observed color deviates farther from red as the transparency of the LM decreases. In the case of the MSG LM, the red color of the LM in the back was barely visible through the yellow LM placed in front (Figure 2B). The MFS LM, on the other hand, showed high transparency, as the red color of the LM in the back clearly showed through the yellow placed in front (Figure 2B). This observation is supported by several reports in the literature which suggest that nanoparticles are likely to form LMs with high transparency.[27,43] In the case of LMs made with MIX, the yellow LM, placed in front, appeared orange, indicating transparency but to a lesser degree than the MFS LM (Figure 2B). The lowest transparency of the MSG LM can be explained based on the larger particle size of SG since coatings containing larger particles are known to scatter light and thus interfere with light transmittance.[47] The reason behind MIX particles showing higher transparency than the MSG can be understood based on microscopy images (Figure 1B) which showed the entire LM to be covered with a fine coating of the MFS while the MSG particles are distributed more sparsely. Since the MSG particles do not seem to form a dense layer on the surface of the MIX LM, they are not expected to interfere with light transmittance significantly.

Quantitative estimation of the transparency of the three different types of LMs was also performed by analyzing the background blue color transmitted through the colorless LMs (Figure 2C). The background blue color transmission will be affected by the type of coating; a higher transmittance signifies higher transparency. The MSG LMs appeared less transparent than the other two LMs as blue color transmission was low. The other two LMs, MFS and MIX, showed comparable transmission of the blue color. The results obtained are in agreement with the qualitative observations.

Coalescence. While coalescence of LMs has been exploited by researchers for microfluidic functions such as mixing of reagents and consequent chemical reactions,[11,17,30,48−50] our aim in this work is to design LMs stable against coalescence such that they can be stacked in a jar to be used as single assay reagent reservoirs for in-field analyses without the need for dispensing equipment such a pipette. As discussed previously, transparent and coalescence-resistant LMs will also be useful for cell culture applications and other chemical analyses. The hydrophobicity, thickness,[51] and particle size[30,44] of the coating have been indicated to play a role in LM coalescence. The resistance of the LMs to coalescence was studied by (i) stacking multiple LMs in a 500 μL polypropylene microcentrifuge tube and (ii) placing multiple LMs side by side in a polystyrene vial and shaking the vial to allow the LMs to come in contact. In both cases, the MFS LMs coalesced immediately, while two LMs made from the MIX or MSG did not (Figure 1A; videos of coalescence have been provided in Supporting Information S1, S2, and S5). MIX LMs behave similarly to MSG LMs with respect to coalescence. The microscopic examination of MIX LMs shows them coated with MFS with interspersed MSG particles. The MSG particles, in this case, were located farther from each other than in the MSG LM, where the entire surface was covered with MSG (Figure 1B,C). However, it seems that the reinforcing effect of a few MSG particles is sufficient for the MIX-coated LM to exhibit resistance to coalescence.

Since the silane attached to SG (TFOS) is more hydrophobic than the one attached to the FS (hexamethyldisilazane), it can be assumed that MSG is more hydrophobic.[29,51] Also, the larger MSG particles are more likely to form a thicker, less uniform coating (Figure 1B,C). Thus, the differences observed in the coalescence behavior of the differently coated LMs led to the question of whether the hydrophobicity of MSG, its larger particle size, or both together render these LMs resistant to coalescence. Thus, we modified FS with the same silane, TFOS, that was attached to the SG and confirmed the attachment by FTIR analysis (Supporting Information Figure

https://doi.org/10.1021/acsami.4c14949
ACS Appl. Mater. Interfaces 2024, 16, 68336−68347

S2). This preparation of FS (T8-MFS) provided a hydrophobic coating with the same hydrophobicity as that of MSG and the same particle size as that of MFS (CAB-O-SIL). When two LMs formed using T8-MFS were subjected to the coalescence study as described above, they coalesced instantly (similar to the MFS-coated LMs; Figure 3, video of coalescence has been provided in Supporting Information, S6). This result strongly indicates that the resistance to coalescence demonstrated by the MSG-coated LMs was a function of the particle size of the MSG rather than its higher hydrophobicity.

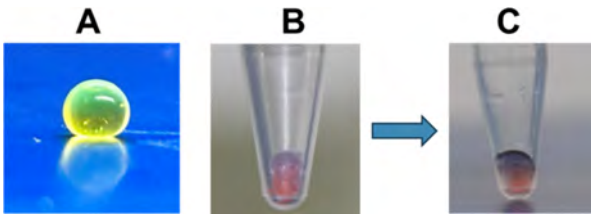

Figure 3. (A) LM fabricated with TFOS-linked FS (T8-MFS) as the hydrophobic coating showed a transparency similar to the MFS LM. (B) Coalescence behavior of T8-MFS: a T8-MFS coated LM, fabricated with blue-colored water, was placed on top of a similarly coated red-colored LM in a 500 μL microcentrifuge tube. (C) The second LM can be seen fused to the first one.

Expandability of the LM and Resistance to Poking. The ability of LMs to be injected and expand without collapsing or deforming, even without excess coating powder, is crucial for their use as microreactors.[20,52] The LMs fabricated in this study were thus characterized for these properties. Poking with the polypropylene pipet tip did not deform or destabilize any of the three LMs. However, the MSG LMs sometimes deformed while being manipulated with a plastic spatula. To examine their expandability, the three types of LMs were prepared with 5 μL of yellow-colored DW and injected repeatedly with red-colored DW until they collapsed or filled up the microwell (Figure 4A). The use of colored DW facilitated observation of the expansion of the LM. The 5 μL MFS and MIX LMs could be injected with up to 100 μL red-colored DW (in increments) without the loss of their structural integrity. While the MSG LMs were able to accommodate the first injection of 10 μL red DW, the next 10 μL injection caused them to collapse, as can be seen by the water droplet sticking to the side of the well in Figure 4A. These observations indicate that the MFS and MIX LMs, during their fabrication, gather enough FS particles to form multiple layers of coating, which allow the LMs to reseal (also known as self-heal[20]) upon expansion. However, the MSG particles are not able to reorganize and reseal the LM. This could be because MFS, being a fine powder, forms multiple uniform layers on the LM surface as depicted in the cartoon (Figure 1C). Consequently, upon expansion, particles from the multilayers are brought to the liquid/solid interface causing the LM to reseal easily.[26,53] On the other hand, the MSG LMs, due to their larger particle size, may not get coated with a uniform layer and produce bigger interstitial pores in the coating (Figure 1C). The size of the MSG particles will then make it more difficult for the particles from other layers (if present) to fit into and fill in the expanding gaps at the liquid/solid interface.

Stability. While the small volumes of LMs offer the advantage of accelerated reaction rates and reduced reagent usage, the microliter volumes[27,31,54] also limit their use due to the rapid evaporation of the encapsulated liquid. Most LMs exhibit slower evaporation of encapsulated liquids compared to corresponding free droplets[54] but subjecting these LMs to high temperatures still poses a challenge. For LMs to be used for colorimetric assays, they should be stable for the duration of the assays, which can be up to 30 min or more after the analyte has been injected. The assays can also require incubation at different temperatures, typically up to 37 °C. Buckling time[31] (time at which LM begins to deform due to evaporation of internal liquid) and evaporation time (time at which the entire internal liquid of the LM has evaporated) are known to be affected by the size of the coating particles, the number of particle layers in the coating, and the chemical nature of the coating.[3,27,31] Buckling has been observed to occur sooner in LMs formed from microparticles than those formed from nanoparticles.[7,26,43] Larger particles form more porous coatings due to bigger interstitial voids between particles, which leads to more rapid evaporation of the inner liquid[55,56] (Figure 1C). Given the differences in particle size of the coatings used in this study, the evaporation of each of the three different LMs was studied at three different temperatures (4 °C, RT (26 °C), and 37 °C) (Figure 4B). All three LMs are more stable at 4 °C than at higher temperatures, as it takes much longer for them to buckle and evaporate at this low temperature. As expected, the MFS and MIX LMs evaporated significantly more slowly than the MSG LMs. Figure S3 (Supporting Information) summarizes the buckling and evaporation times for all three LMs at RT (26 °C) (videos of evaporation of LMs at 26 and 37 °C have been provided in Supporting Information S3 and S7, respectively). Humidity was observed to affect the evaporation and buckling times significantly (Table 1) as LMs evaporated much more slowly at high RH (78%) at 26 °C similar to what has been reported by other researchers.

The images of LMs taken during evaporation at different temperatures were analyzed to measure the decrease in volume at different time periods (0−45 min; Figure 4C). At the lowest temperature (4 °C), the MSG LMs showed the most rapid decrease in volume over time, indicating poor ability to retain the liquid. MIX LMs performed better than MSG LMs but still experienced a notable decline in volume, especially in the first 5−10 min. MFS LMs showed the slowest decrease in volume and hence the highest resistance to the loss of liquid through evaporation. At intermediate temperature (26 °C), the MFS LMs were still the slowest to evaporate, but the gap between the performance of MIX and MSG was more pronounced at this temperature. At 37 °C, all LMs showed an accelerated loss of volume, but the MFS LMs persisted as the ones with the highest resistance to evaporation and the MIX LMs showed a moderate behavior. This effectiveness of MFS coating in both MFS and MIX LMs is due to the presence of smaller particles which create a denser layer, reducing the size of interstitial pores and thus slowing down the evaporation (Figure 4B). While the initial resistance of the MIX LMs to loss of volume is inferior to that of the MFS LMs, they exhibit evaporation and buckling times similar to the MFS LMs (Figures 4B and S3 (Supporting Information)). It is possible that as volume decreases, the excess MFS particles redistribute on the surface of MIX LMs to form multiple layers, causing the evaporation to slow down eventually, while the MIX LMs do not have this advantage. Microscopic examination showed that MIX LMs

https://doi.org/10.1021/acsami.4c14949
ACS Appl. Mater. Interfaces 2024, 16, 68336−68347

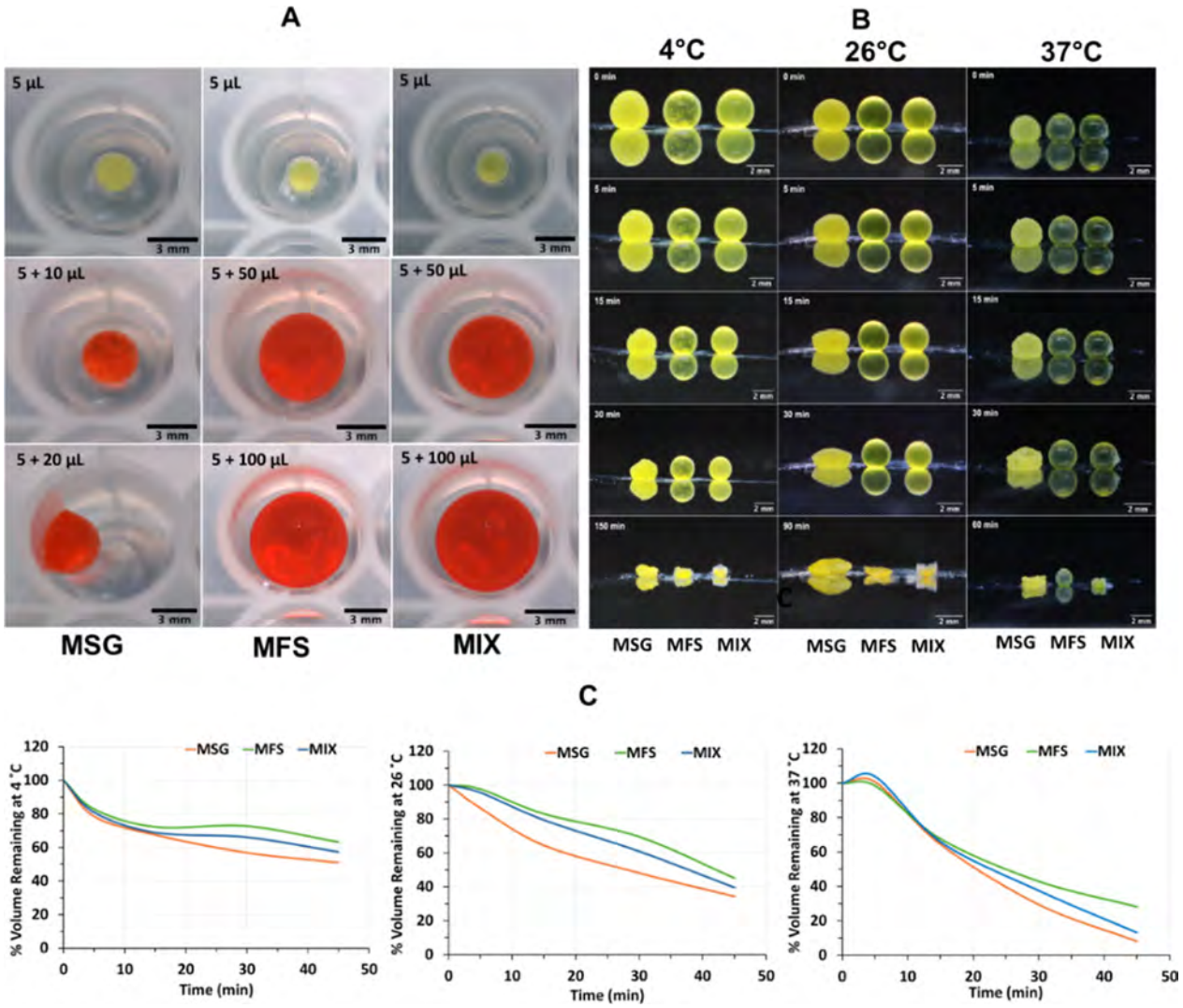

Figure 4. Mechanical and thermal properties of LMs made from three different hydrophobic powders, MSG, MFS, and MIX (in order from left to right). (A) Expandability of LMs was determined by injecting the 5 μL yellow-colored LM of each type with red-colored water. The MFS and MIX LMs were able to reseal up to an expansion in volume of at least 20 times, while the MSG LMs collapsed after an expansion of three times. (B) LMs were allowed to evaporate by standing at different temperatures. Differences in stability of the different marbles at different temperatures can be observed from the differences in time when each starts buckling and when complete evaporation of internal liquid occurs. (C) Change in volume of LMs on standing at different temperatures was calculated using images captured at different time points. The volume of the originally fabricated LM at time zero was designated as 100% and the remaining volume % at later time points was calculated for each LM as (volume at any time point/volume at time zero × 100). The type of coating and temperature at which LM was stored affected the rate and pattern of evaporation but the MFS-coated LMs showed higher resistance to evaporation at all temperatures tested.

are coated uniformly with MFS and that the big MSG particles are interspersed sparsely. These findings support the hypothesis of Tenjimbayashi et al., who proposed that a balance between small and large particles can enhance LM stability and control evaporation rates. The enhancement is achieved by having smaller particles fill the gaps between bigger particles,[57] creating a denser layer. This explains the stability of MIX LMs against coalescence similar to MSG LMs and a resistance to evaporation comparable to that of MFS LMs. All three LMs exhibited evaporation times longer than those of the bare liquid droplet. Thus, based on the argument made by Laborie et al., it can be concluded that all three LMs are coated with multiple layers of the coating particles.[57] While many prior studies indicate that the buckling time is affected by the coating particle size and/or the number of particle layers, Cengiz and Erbil observed an inverse relationship between the hydrophobicity of the coating and the buckling time of the LM.[26] Our results agree with this observation given that the MSG coating is more hydrophobic, and LMs made with MSGs buckle and evaporate faster.

Colorimetric Assays in LMs. Their excellent transparency, resistance to coalescence, robustness, and stability make the MIX LMs an ideal microreactor to perform colorimetric assays (Figure 5). When MIX LMs were placed in polystyrene microwell plates, the LMs shed some of their coating which interfered with the reading of absorbance in a microwell plate reader. We have previously used a smartphone application to quantify color intensities in colorimetric assays, but the app does not work well with samples in a transparent plastic plate as it reflects light, thus affecting the quality of images. Hence, for performing these assays, MIX LMs were placed in opaque CA microwell plates fabricated in our laboratory.[41]

https://doi.org/10.1021/acsami.4c14949
ACS Appl. Mater. Interfaces 2024, 16, 68336−68347

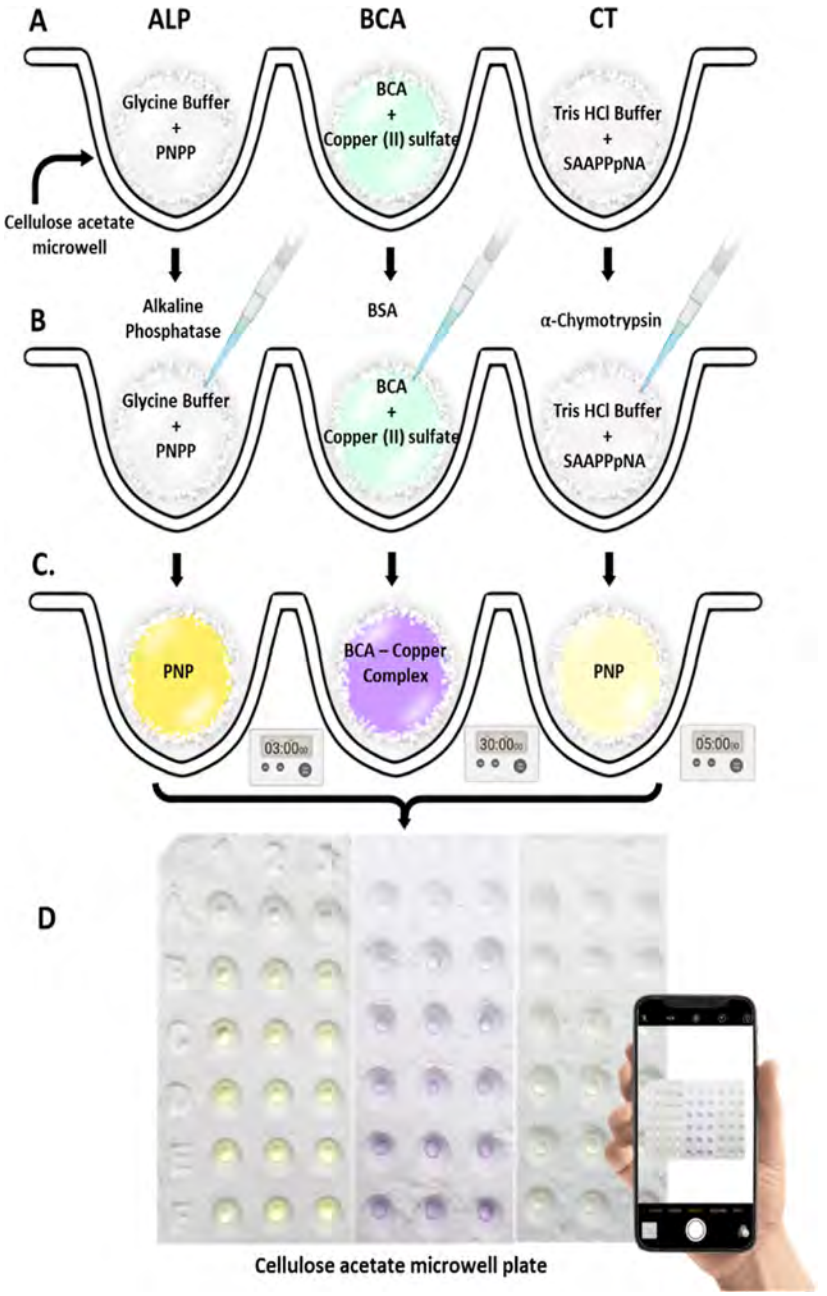

Figure 5. Design for performance of colorimetric assays in LMs prepared with MIX as the coating (created with BioRender.com). (A) MIX LMs were formed using reagents for the ALP, BCA, and CT assays and placed in separate wells (from left to right) in a CA microwell plate. (B) Each LM was then injected with the respective analyte (AP, BSA, and CT from left to right). (C) The ensuing reaction in each LM led to the appearance of a color proportional to the analyte concentration. (D) Color intensities in each LM were measured using a smartphone application (Spotxel).

Three different colorimetric methods were performed in two systems: (i) classic 96-well polystyrene plates using a microplate reader for quantification of color intensities as a point of reference and (ii) LMs placed in a 96-well CA plate template using the Spotxel application as the color intensity quantifying tool. The LMs in each assay were fabricated by rolling a droplet containing all reagents needed for each assay (e.g., substrate, buffer, etc.) on a bed of the coating powder (MFS, MSG or MIX). Figure 5 shows LMs with the assay mixtures placed in CA microwell plates. The assay for AP activity is based on hydrolysis of PNPP by AP resulting in the formation of a yellow product (*p*-nitrophenol; PNP). The enzyme activity is directly proportional to the amount of PNP formed, which was quantified by measuring the absorbance of the reaction mixture at 405 nm and its color intensity. Different dilutions of the enzyme solution were used in the reaction mixture to generate a standard curve for AP activity. PNP formation was observed to be directly proportional to AP concentration used as can be observed in Figure 6B1. BCA is a routinely used colorimetric method for protein quantification. It is based on a purple-colored complex formation between proteins, Cu(II) ions, and the BCA. The protein concentration is directly proportional to the intensity of purple color formed, which can be quantified by measuring the absorbance of the reaction mixture at 562 nm or its color intensity. Figure 6B1–B3 shows the standard plots for the BCA method in the two

https://doi.org/10.1021/acsami.4c14949
ACS Appl. Mater. Interfaces 2024, 16, 68336–68347

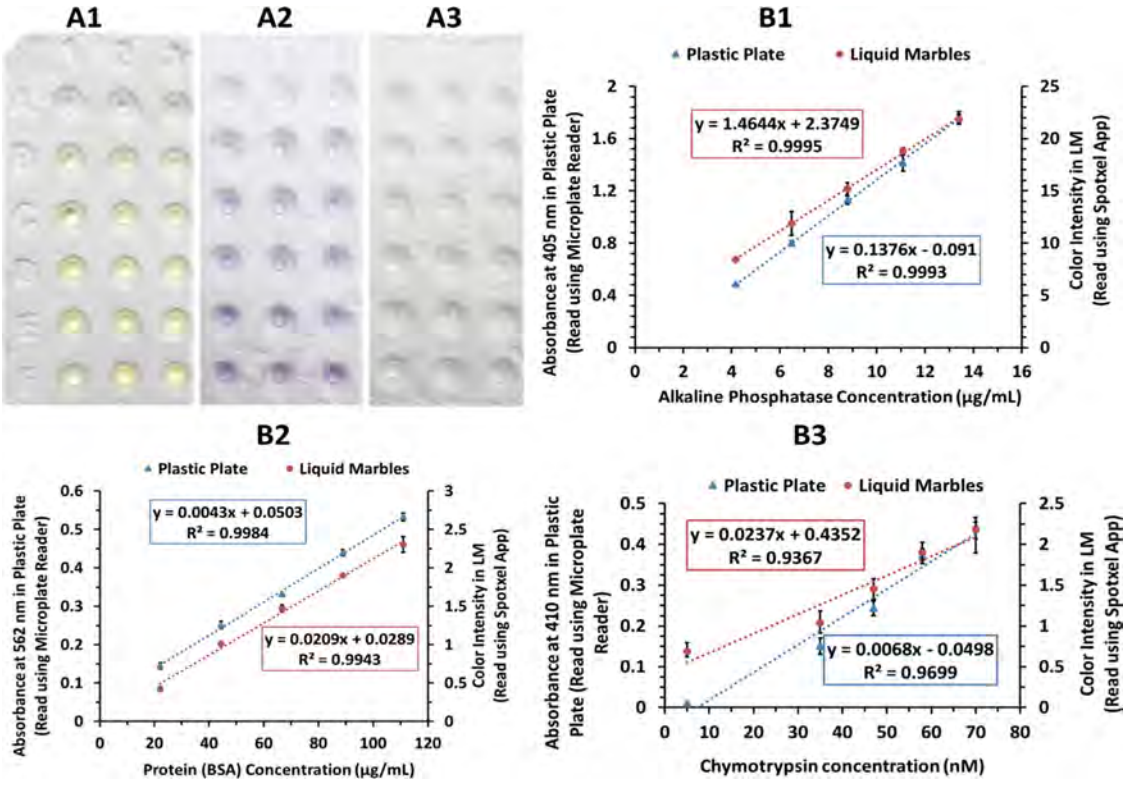

Figure 6. Results from colorimetric assays performed in LMs placed in CA plates: MIX LM were used to perform (A1) AP assay (hydrolysis of *p*-nitrophenyl phosphate); (A2) BCA assay; and (A3) CT assay (hydrolysis of *N*-succinyl-Ala-Ala-Pro-Phe-*p*-nitroanilide). Plots (B1−B3) show quantitative analysis of results obtained for each of the three colorimetric assays (AP assay, BCA assay, and CT assay, respectively) in both plastic microwell plates and in MIX LMs placed in CA microwell plates. The linear correlation coefficients for each assay were comparable in the two systems.

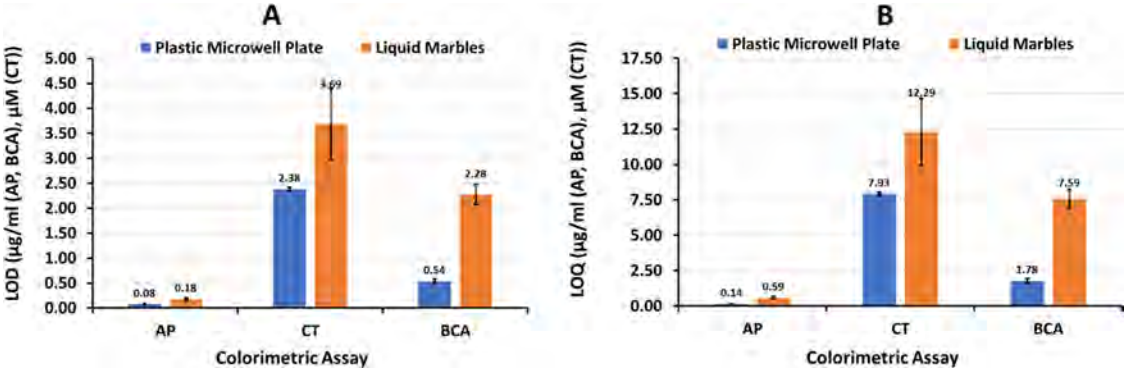

Figure 7. Comparison of the colorimetric assay in LMs with that in polystyrene microwell plates. (A) LOD and (B) LOQ for the three colorimetric assays: AP assay, BCA assay, and CT assay, in both plastic microwell plates and in the MIX LMs placed in CA microwell plates. Standard analyte activity or concentration plots were prepared, and linear regression performed to obtain value of the slope. The LOD was then calculated using the formula: 3σ/slope, and the LOQ was calculated as 10σ/slope.

systems. Different dilutions of BSA were allowed to react with the same amounts of BCA reagents and resulted in a standard linear plot where the purple-colored complex formation showed a linear increase with an increase in the protein concentration in both systems. The assay used for measuring CT activity involves CT-catalyzed hydrolysis of the chromogenic substrate *N*-succinyl-Ala-Ala-Pro-Phe-*p*-nitroanilide (SAAPPpNA).[40] This reaction results in the formation of a yellow product, *p*-nitroaniline (PNA). The quantity of PNA formed was monitored by measuring the absorbance at 410 nm or its color intensity. Figure 6 shows the results obtained when different dilutions of CT were added to the assay mixtures containing identical amounts of SAAPPpNA. PNA formation was observed to be directly proportional to the quantity of CT added in both systems tested.

As can be determined from the linear correlation coefficients in each case (Figure 6), the linearity of the method using the LM and Spotxel Reader gave an accuracy comparable to the standard system based on polystyrene plates and a microplate reader. Based on the limit of detection (LOD) and limit of quantification (LOQ) values determined for each assay in each of the two systems (Figure 7), the polystyrene plate system coupled to a microplate reader is better for detecting and quantifying lower concentrations than the LMs. Nevertheless,

https://doi.org/10.1021/acsami.4c14949
ACS Appl. Mater. Interfaces 2024, 16, 68336−68347

the differences are small (1.5−4-fold). The slopes for assays in LMs are consistently bigger because the app measures the color intensities while polystyrene plates are read using a microplate reader which measures absorbances. The color intensities are expressed by the app on a scale different from the absorbance by a microplate reader; hence, the slopes must not be used in this study as a measure of the sensitivity of the assays. The CT and AP assays have very short incubation times (3−5 min) at RT. The evaporation experiments showed that there was no significant change in the LM size at RT in 3−5 min, and hence, the change in volume of the LM is not of concern for these assays. The BCA assay, however, requires 30 min incubation at 37 °C, and the LMs shrink to approximately 40% of their original size under these conditions (Figure 4). As discussed in the stability study section, this shrinkage can be prevented by performing the assay under higher-humidity conditions. Interestingly, the linearity of assays was not affected by the change in volume of the LM as observed from multiple repetitions of the assay. This is most likely because the shrinkage occurred in all the LMs carrying the different concentrations of protein, and hence, the effect was systematic. Nevertheless, this factor must be considered when an analysis in the LM is designed at relatively high temperatures.

Performing colorimetric assays in the optimized MIX LMs is simple and rapid. A significant reduction in waste generation from each assay, without compromising on the quality, makes them an appealing tool for colorimetric assays and other chemicals/biochemical analyses. Coupled to smartphone applications, the use of LMs for colorimetric assays offers an analytical tool free of any sophisticated laboratory infrastructure or expensive instruments.

CONCLUSIONS

Highly stable, transparent, and expandable LMs were fabricated for colorimetric assays using a hybrid coating of silanized fumed silica (MFS) and silanized silica gel (MSG). Smaller (nanosized) particles (MFS) favor higher transparency, expandability, and lower evaporation rates, while bigger (microsized) particles (MSG) make LMs resistant to coalescence. Through MIX LMs, the study provides evidence that particles of differing hydrophobicity and sizes complement each other in a surface coating (MIX of MSG and MFS in a w/w ratio of 3:7 in this case) and thus offer an effective way to fabricate LMs fine-tuned to specific applications.[27] The LMs were formed as microreactors containing all of the assay reagents in one drop of 10 μL; additional analytes could be easily injected into these LMs without compromising their integrity. Each of the three different colorimetric assays performed in MIX LMs allowed the detection of low concentrations of the analytes, as evidenced by the LOD values (AP: 0.18 μg/mL; BSA: 2.28 μg/mL; CT: 3.69 μM) with high accuracy and precision. The use of LMs reduces chemical waste generation as smaller reagent volumes inside LMs are slower to evaporate when compared with naked droplets in the microwell plate. This is particularly relevant in assays that require long incubation periods. The use of prefabricated LMs for detecting/quantifying the analyte through a smartphone application also makes the process accessible outside typical laboratory settings, which offers a great advantage for on-site analysis of samples.

ASSOCIATED CONTENT

Supporting Information

The Supporting Information is available free of charge at https://pubs.acs.org/doi/10.1021/acsami.4c14949.

FTIR spectra of MSG; FTIR spectra of T8-modified fumed silica (T8-MFS); and graphic demonstrating the stability of LMs prepared from three different hydrophobic powders observed at RT (26 °C) at 49% RH (PDF)

Coalescence behavior of MFS LMs (MP4)

Coalescence behavior of MSG LMs (MOV)

Effect of surface coating on evaporation of LMs at 26 °C (MP4)

Coalescence behavior of MIX LMs (4MSG: 6MFS w/w) (MOV)

Coalescence behavior MIX LMs (3MSG: 7MFS w/w) (MOV)

Coalescence behavior of T8-MFS LMs (MP4)

Effect of surface coating on evaporation of LMs at 37 °C (MOV)

AUTHOR INFORMATION

Corresponding Author

Vibha Bansal − *Department of Chemistry, University of Puerto Rico at Cayey, Cayey, Puerto Rico 00736, United States;* orcid.org/0000-0003-4024-9882; Email: vibha.bansal@upr.edu

Authors

Renis Agosto Nieves − *Department of Chemistry, University of Puerto Rico at Cayey, Cayey, Puerto Rico 00736, United States;* Present Address: Department of Systems Pharmacology and Translational Therapeutics, Perelman School of Medicine, University of Pennsylvania, 231S, 34th Street, Philadelphia, PA 19104-6323, USA

Gabriela Gomez Dopazo − *Department of Chemistry, University of Puerto Rico at Cayey, Cayey, Puerto Rico 00736, United States; Department of Chemical & Biomolecular Engineering, University of Pennsylvania, Philadelphia, Pennsylvania 19104-6323, United States*

Joseph Rosenfeld − *Department of Chemical & Biomolecular Engineering, University of Pennsylvania, Philadelphia, Pennsylvania 19104-6323, United States*

Hong-Huy Tran − *Department of Chemical & Biomolecular Engineering, University of Pennsylvania, Philadelphia, Pennsylvania 19104-6323, United States*

Lyanivette Alvarado Lopez − *Department of Biology, University of Puerto Rico at Cayey, Cayey, Puerto Rico 00736, United States*

Jose Sotero-Esteva − *Department of Mathematics, University of Puerto Rico at Humacao, Humacao, Puerto Rico 00791, United States*

Ezio Fasoli − *Department of Chemistry, University of Puerto Rico at Humacao, Humacao, Puerto Rico 00791, United States*

Ivan J. Dmochowski − *Department of Chemistry, University of Pennsylvania, Philadelphia, Pennsylvania 19104-63223, United States;* orcid.org/0000-0001-7162-1347

Daeyeon Lee − *Department of Chemical & Biomolecular Engineering, University of Pennsylvania, Philadelphia, Pennsylvania 19104-6323, United States;* orcid.org/0000-0001-6679-290X

https://doi.org/10.1021/acsami.4c14949
ACS Appl. Mater. Interfaces 2024, 16, 68336−68347

Complete contact information is available at:
https://pubs.acs.org/10.1021/acsami.4c14949

Author Contributions

The manuscript was written through contributions of all authors. All authors have given approval to the final version of the manuscript.

Funding

This project was supported by the National Science Foundation grant, NSF-DMR-2122102 and Penn MRSEC, NSF-2309043. Support was also received from Instrumentation facilities created through Institutional Development Award (IDeA) from the National Institute of General Medical Sciences of the National Institutes of Health under grant number P20 GM103475. The contents of this manuscript are solely the responsibility of the authors and do not necessarily represent the official view of the NSF or NIH.

Notes

The authors declare no competing financial interest.

■ ACKNOWLEDGMENTS

The authors sincerely acknowledge the help of Nathalia Liu-Derestrepo and Luis A. Delgado Rodriguez in recording the coalescence video of MIX (6MFS:4MSG w/w) LMs.

■ REFERENCES

(1) Kamiya, N.; Ohama, Y.; Minamihata, K.; Wakabayashi, R.; Goto, M. Liquid Marbles as an Easy-to-Handle Compartment for Cell-Free Synthesis and In Situ Immobilization of Recombinant Proteins. *Biotechnol. J.* **2018**, *13* (12), 1800085.
(2) Avrămescu, R. E.; Ghica, M.-V.; Dinu-Pîrvu, C.; Udeanu, D. I.; Popa, L. Liquid Marbles: From Industrial to Medical Applications. *Molecules* **2018**, *23* (5), 1120.
(3) Aussillous, P.; Quéré, D. Liquid Marbles. *Nature* **2001**, *411* (6840), 924−927.
(4) Oliveira, N. M.; Reis, R. L.; Mano, J. F. The Potential of Liquid Marbles for Biomedical Applications: A Critical Review. *Adv. Healthcare Mater.* **2017**, *6* (19), 1700192.
(5) Zhao, Z.; Yao, X.; Zhao, W.; Shi, B.; Sridhar, S.; Pu, Y.; Pramana, S.; Wang, D.; Wang, S. Highly Transparent Liquid Marble in Liquid (HT-LMIL) as 3D Miniaturized Reactor for Real-Time Bio-/Chemical Assays. *Chem. Eng. J.* **2022**, *443*, 136417.
(6) Ooi, C. H.; Jin, J.; Sreejith, K. R.; Nguyen, A. V.; Evans, G. M.; Nguyen, N.-T. Manipulation of a Floating Liquid Marble Using Dielectrophoresis. *Lab Chip* **2018**, *18* (24), 3770−3779.
(7) Ooi, C. H.; Vadivelu, R.; Jin, J.; Sreejith, K. R.; Singha, P.; Nguyen, N.-K.; Nguyen, N.-T. Liquid Marble-Based Digital Microfluidics—Fundamentals and Applications. *Lab Chip* **2021**, *21* (7), 1199−1216.
(8) Ooi, C. H.; Nguyen, N.-T. Manipulation of Liquid Marbles. *Microfluid. Nanofluid.* **2015**, *19* (3), 483−495.
(9) Jin, J.; Huang, Z.; Xie, Y.; Shen, Z.; Liu, B.; Chen, H. Fabrication of Stable Monolayer Liquid Marbles with Reduced Particle Coverage and Locomotion on Hydrophilic Surface. *Commun. Mater.* **2024**, *5* (1), 64.
(10) Nguyen, N.; Singha, P.; Zhang, J.; Phan, H.; Nguyen, N.; Ooi, C. H. Digital Imaging-based Colourimetry for Enzymatic Processes in Transparent Liquid Marbles. *ChemPhysChem* **2021**, *22* (1), 99−105.
(11) Zhao, Z.; Qin, S.; Wang, D.; Pu, Y.; Wang, J.-X.; Saczek, J.; Harvey, A.; Ling, C.; Wang, S.; Chen, J.-F. Multi-Stimuli-Responsive Liquid Marbles Stabilized by Superhydrophobic Luminescent Carbon Dots for Miniature Reactors. *Chem. Eng. J.* **2020**, *391*, 123478.
(12) Sarvi, F.; Arbatan, T.; Chan, P. P. Y.; Shen, W. A Novel Technique for the Formation of Embryoid Bodies Inside Liquid Marbles. *RSC Adv.* **2013**, *3* (34), 14501.
(13) Bormashenko, E.; Balter, R.; Aurbach, D. Micropump Based on Liquid Marbles. *Appl. Phys. Lett.* **2010**, *97* (9), 091908.
(14) Fujii, S.; Yusa, S.; Nakamura, Y. Stimuli-Responsive Liquid Marbles: Controlling Structure, Shape, Stability, and Motion. *Adv. Funct. Mater.* **2016**, *26* (40), 7206−7223.
(15) Nguyen, N.-K.; Tran, D. T.; Chuang, A.; Singha, P.; Kijanka, G.; Burford, M.; Ooi, C. H.; Nguyen, N.-T. Liquid Marble—A High-Yield Micro-Photobioreactor Platform. *React. Chem. Eng.* **2023**, *8* (11), 2710−2716.
(16) Ferronato, G. D. A.; Dos Santos, C. M.; Rosa, P. M. D. S.; Bridi, A.; Perecin, F.; Meirelles, F. V.; Sangalli, J. R.; Da Silveira, J. C. Bovine In Vitro Oocyte Maturation and Embryo Culture in Liquid Marbles 3D Culture System. *PLoS One* **2023**, *18* (4), No. e0284809.
(17) Vadivelu, R. K.; Kamble, H.; Munaz, A.; Nguyen, N.-T. Liquid Marbles as Bioreactors for the Study of Three-Dimensional Cell Interactions. *Biomed. Microdevices* **2017**, *19* (2), 31.
(18) Sun, J.; Xu, Y.; Pan, W.; Hu, Y.; He, Z.; Xu, W.; Song, J. Oily Wastewater Detector Based on Superhydrophobic Liquid Marbles. *Colloids Surf., A* **2024**, *692*, 134030.
(19) Li, N.; Wanyan, H.; Lu, S.; Xiao, H.; Zhang, M.; Liu, K.; Li, X.; Du, B.; Huang, L.; Chen, L.; Ni, Y.; Wu, H. Robust Cellulose-Based Hydrogel Marbles with Excellent Stability for Gas Sensing. *Carbohydr. Polym.* **2023**, *306*, 120617.
(20) Oliveira, N. M.; Correia, C. R.; Reis, R. L.; Mano, J. F. Liquid Marbles for High-Throughput Biological Screening of Anchorage-Dependent Cells. *Adv. Healthcare Mater.* **2015**, *4* (2), 264−270.
(21) McHale, G.; Newton, M. I. Liquid Marbles: Topical Context within Soft Matter and Recent Progress. *Soft Matter* **2015**, *11* (13), 2530−2546.
(22) Aalders, J.; Léger, L.; Piras, D.; Van Hengel, J.; Ledda, S. Use of Transparent Liquid Marble: Microbioreactor to Culture Cardiospheres. In *Next Generation Culture Platforms for Reliable In Vitro Models*; Brevini, T. A. L., Fazeli, A., Turksen, K., Eds.; *Methods in Molecular Biology*; Springer US: New York, NY, 2021; Vol. *2273*, pp 85−102..
(23) Li, H.; Liu, P.; Kaur, G.; Yao, X.; Yang, M. Transparent and Gas-Permeable Liquid Marbles for Culturing and Drug Sensitivity Test of Tumor Spheroids. *Adv. Healthcare Mater.* **2017**, *6* (13), 1700185.
(24) Lin, K.; Chen, R.; Zhang, L.; Zang, D.; Geng, X.; Shen, W. Transparent Bioreactors Based on Nanoparticle-Coated Liquid Marbles for In Situ Observation of Suspending Embryonic Body Formation and Differentiation. *ACS Appl. Mater. Interfaces* **2019**, *11* (9), 8789−8796.
(25) Roy, P. K.; Binks, B. P.; Bormashenko, E.; Legchenkova, I.; Fujii, S.; Shoval, S. Manufacture and Properties of Composite Liquid Marbles. *J. Colloid Interface Sci.* **2020**, *575*, 35−41.
(26) Cengiz, U.; Erbil, H. Y. The Lifetime of Floating Liquid Marbles: The Influence of Particle Size and Effective Surface Tension. *Soft Matter* **2013**, *9* (37), 8980.
(27) Fullarton, C.; Draper, T. C.; Phillips, N.; Mayne, R.; De Lacy Costello, B. P. J.; Adamatzky, A. Evaporation, Lifetime, and Robustness Studies of Liquid Marbles for Collision-Based Computing. *Langmuir* **2018**, *34* (7), 2573−2580.
(28) Sun, Y.; Zheng, Y.; Liu, C.; Zhang, Y.; Wen, S.; Song, L.; Zhao, M. Liquid Marbles, Floating Droplets: Preparations, Properties, Operations and Applications. *RSC Adv.* **2022**, *12* (24), 15296−15315.
(29) Kulkarni, S. A.; Ogale, S. B.; Vijayamohanan, K. P. Tuning the Hydrophobic Properties of Silica Particles by Surface Silanization Using Mixed Self-Assembled Monolayers. *J. Colloid Interface Sci.* **2008**, *318* (2), 372−379.
(30) Jin, J.; Ooi, C.; Dao, D.; Nguyen, N.-T. Coalescence Processes of Droplets and Liquid Marbles. *Micromachines* **2017**, *8* (11), 336.
(31) Sreejith, K. R.; Ooi, C. H.; Dao, D. V.; Nguyen, N.-T. Evaporation Dynamics of Liquid Marbles at Elevated Temperatures. *RSC Adv.* **2018**, *8* (28), 15436−15443.
(32) Pan, M.; Rosenfeld, L.; Kim, M.; Xu, M.; Lin, E.; Derda, R.; Tang, S. K. Y. Fluorinated Pickering Emulsions Impede Interfacial Transport and Form Rigid Interface for the Growth of Anchorage-

Dependent Cells. *ACS Appl. Mater. Interfaces* **2014**, *6* (23), 21446−21453.
(33) Šiffalovič, P.; Jergel, M.; Benkovičová, M.; Vojtko, A.; Nádaždy, V.; Ivančo, J.; Bodík, M.; Demydenko, M.; Majková, E. Towards New Multifunctional Coatings for Organic Photovoltaics. *Sol. Energy Mater. Sol. Cells* **2014**, *125*, 127−132.
(34) McEleney, P.; Walker, G. M.; Larmour, I. A.; Bell, S. E. J. Liquid Marble Formation Using Hydrophobic Powders. *Chem. Eng. J.* **2009**, *147* (2−3), 373−382.
(35) Destino, J. F.; Cunningham, K. At-Home Colorimetric and Absorbance-Based Analyses: An Opportunity for Inquiry-Based, Laboratory-Style Learning. *J. Chem. Educ.* **2020**, *97* (9), 2960−2966.
(36) Ihrke, I. Opacity. In *Computer Vision*; Springer International Publishing: Germany, 2021; pp 1−6..
(37) Harris, C. R.; Millman, K. J.; Van Der Walt, S. J.; Gommers, R.; Virtanen, P.; Cournapeau, D.; Wieser, E.; Taylor, J.; Berg, S.; Smith, N. J.; Kern, R.; Picus, M.; Hoyer, S.; Van Kerkwijk, M. H.; Brett, M.; Haldane, A.; del Río, J. F.; Wiebe, M.; Peterson, P.; Gérard-Marchant, P.; Sheppard, K.; Reddy, T.; Weckesser, W.; Abbasi, H.; Gohlke, C.; Oliphant, T. E. Array Programming with NumPy. *Nature* **2020**, *585* (7825), 357−362.
(38) Olson, B. J. S. C. Assays for Determination of Protein Concentration. *Curr. Protoc. Pharmacol.* **2016**, *73* (1), A.3A.1−A.3A.32.
(39) Chen, X.; Chen, J.; Zhang, H.-Y.; Wang, F.-B.; Wang, F.-F.; Ji, X.-H.; He, Z.-K. Colorimetric Detection of Alkaline Phosphatase on Microfluidic Paper-Based Analysis Devices. *Chin. J. Anal. Chem.* **2016**, *44* (4), 591−596.
(40) Jaworek, M. W.; Winter, R. Exploring Enzymatic Activity in Multiparameter Space: Cosolvents, Macromolecular Crowders and Pressure. *ChemSystemsChem* **2021**, *3* (2), No. e2000029.
(41) Gomez-Dopazo, G. B.; Agosto-Nieves, R. J.; Albarracin Rivera, R. L.; Colon Morera, S. M.; Nazario, D. R.; Ramos, I.; Dmochowski, I. J.; Lee, D.; Bansal, V. Cellulose Acetate Microwell Plates for Highthroughput Colorimetric Assays. *RSC Adv.* **2024**, *14*, 15319−15327.
(42) Oliveira, N. M.; Reis, R. L.; Mano, J. F. The Potential of Liquid Marbles for Biomedical Applications: A Critical Review. *Adv. Healthcare Mater.* **2017**, *6* (19), 1700192.
(43) Bhosale, P. S.; Panchagnula, M. V.; Stretz, H. A. Mechanically Robust Nanoparticle Stabilized Transparent Liquid Marbles. *Appl. Phys. Lett.* **2008**, *93* (3), 034109.
(44) Planchette, C.; Biance, A.-L.; Pitois, O.; Lorenceau, E. Coalescence of Armored Interface under Impact. *Phys. Fluids* **2013**, *25* (4), 042104.
(45) Mousavi, M.; Fini, E. Silanization Mechanism of Silica Nanoparticles in Bitumen Using 3-Aminopropyl Triethoxysilane (APTES) and 3-Glycidyloxypropyl Trimethoxysilane (GPTMS). *ACS Sustainable Chem. Eng.* **2020**, *8* (8), 3231−3240.
(46) Li, Y.; Li, L.; Wan, D.; Sha, A.; Li, Y.; Liu, Z. Preparation and Evaluation of a Fluorinated Nano-Silica Superhydrophobic Coating for Cement Pavement. *Constr. Build. Mater.* **2022**, *360*, 129478.
(47) McHale, G.; Newton, M. I. Liquid Marbles: Principles and Applications. *Soft Matter* **2011**, *7* (12), 5473.
(48) Chen, Z.; Zang, D.; Zhao, L.; Qu, M.; Li, X.; Li, X.; Li, L.; Geng, X. Liquid Marble Coalescence and Triggered Microreaction Driven by Acoustic Levitation. *Langmuir* **2017**, *33* (25), 6232−6239.
(49) Liu, Z.; Fu, X.; Binks, B. P.; Shum, H. C. Coalescence of Electrically Charged Liquid Marbles. *Soft Matter* **2017**, *13* (1), 119−124.
(50) Arbatan, T.; Li, L.; Tian, J.; Shen, W. Liquid Marbles as Micro-Bioreactors for Rapid Blood Typing. *Adv. Healthcare Mater.* **2012**, *1* (1), 80−83.
(51) Forny, L.; Pezron, I.; Saleh, K.; Guigon, P.; Komunjer, L. Storing Water in Powder Form by Self-Assembling Hydrophobic Silica Nanoparticles. *Powder Technol.* **2007**, *171* (1), 15−24.
(52) Sneha Ravi, A.; Dalvi, S. Liquid Marbles and Drops on Superhydrophobic Surfaces: Interfacial Aspects and Dynamics of Formation: A Review. *ACS Omega* **2024**, *1*, 3c07657.
(53) Dandan, M.; Erbil, H. Y. Evaporation Rate of Graphite Liquid Marbles: Comparison with Water Droplets. *Langmuir* **2009**, *25* (14), 8362−8367.
(54) Li, X.; Wang, Y.; Huang, J.; Yang, Y.; Wang, R.; Geng, X.; Zang, D. Monolayer Nanoparticle-Covered Liquid Marbles Derived from a Sol-Gel Coating. *Appl. Phys. Lett.* **2017**, *111* (26), 261604.
(55) Janardan, N.; Panchagnula, M. V.; Bormashenko, E. Liquid Marbles: Physics and Applications. *Sadhana* **2015**, *40* (3), 653−671.
(56) Tenjimbayashi, M.; Mouterde, T.; Roy, P. K.; Uto, K. Liquid Marbles: Review of Recent Progress in Physical Properties, Formation Techniques, and Lab-in-a-Marble Applications in Microreactors and Biosensors. *Nanoscale* **2023**, *15* (47), 18980−18998.
(57) Laborie, B.; Lachaussée, F.; Lorenceau, E.; Rouyer, F. How Coatings with Hydrophobic Particles May Change the Drying of Water Droplets: Incompressible Surface versus Porous Media Effects. *Soft Matter* **2013**, *9* (19), 4822.

https://doi.org/10.1021/acsami.4c14949
ACS Appl. Mater. Interfaces 2024, 16, 68336−68347